Effects of Some Material and Experimental Variables on the Slurry Wear Characteristics of Zinc-Aluminum Alloys

B.K. Prasad, O.P. Modi, A.K. Jha, and A.K. Patwardhan

(Submitted 7 May 1999)

In this study, the slurry wear behavior of a zinc-based alloy has been examined by the sample rotation method over a range of traversal speeds and distances. The influence of adding silicon to the alloy system on its wear characteristics has also been examined.

The wear rate of the samples increased with increasing traversal distance initially, attained a peak, and then tended to decrease at longer distances. The initial increase in wear rate with distance was attributed to the indenting effect of the slurry constituents (*i.e.*, liquid droplets and the erodant particles) associated with the corrosive action of the liquid in slurry. On the contrary, factors such as entrapment of the erodant mass as well as the corrosion products in the cavities formed on the specimen surfaces could lead to the decrease in wear rate at longer traversal distances. The existence of silicon particles in the alloy microstructure led to improved wear resistance of the alloy system. This was due to the resistance offered by the hard silicon particles against the impinging action of the slurry constituents. Attainment of the wear rate peak at longer traversal distances in the case of the silicon-containing alloy over the one without the element further substantiated the superior wear resistance offered by the silicon particles. Traversal speed led to higher wear rates irrespective of the test conditions and material composition due to the more severe attack of the medium on the specimen surface. However, the presence of silicon particles in the alloy microstructure offered improved wear resistance (inverse of wear rate).

Keywords distance, erosion-corrosion-abrasion, microstructure-property correlation, slurry wear behavior, traversal speed, zinc-aluminum alloys

1. Introduction

Zinc-aluminum alloys have been observed to be suitable for a variety of engineering applications in place of various ferrous and nonferrous alloys.[1–4] In many of the applications, especially so in mining industries, the components encounter slurry environments.[4,5] It has been observed that, generally, sulphate and chloride ions in water constitute the slurry liquid, while the solid mass therein may be soil/sand. Conventional varieties of zinc-aluminum alloys comprise soft phases such as α and η, which perform well under sliding wear conditions involving low operating temperatures.[6–8] Generation of thermally stable microconstituents through the addition of high melting point elements, *e.g.*, silicon and/or nickel, has been observed to improve the mechanical properties and (sliding) wear response of the alloy system at elevated operating temperatures.[6–8] Further, incorporation of hard (ceramic) second-phase particles in the alloy system has also produced identical effects.[9–15] However, practically, no information exists with regard to the response of the zinc-aluminum alloys in slurry environments in spite of the great potential in this direction. Such an assessment and analysis of the wear characteristics of the alloy system could enable a widening of the range of its applications.

In view of the above, the wear behavior of a zinc-aluminum alloy has been studied in a slurry comprising chloride and sulfate ions in the liquid and sand particles as the solid suspended mass. Tests have been conducted over a range of traversal speeds and distances using the sample rotation method. The influence of adding silicon particles on the wear behavior of the alloy system has also been studied. The wear response of the samples has been substantiated through their wear surface and subsurface characteristics.

B.K. Prasad, O.P. Modi, and **A.K. Jha**, Regional Research Laboratory (CSIR), Near Habibganj Naka, Bhopal - 462 026, India. **A.K. Patwardhan**, Metallurgical Engineering Department, University of Roorkee, Roorkee - 247 667, India.

2. Experimental

2.1 Alloy Preparation

The alloys (Table 1) for conducting the experiments were prepared *via* the liquid metallurgy route in the form of 20 mm diameter, 150 mm long cylindrical castings. Cast iron molds were used for solidifying the alloy melt in the required shape and size.

2.2 Slurry Wear Tests

Slurry wear tests were conducted on 15 mm diameter, 10 mm thick samples using the sample rotation method. Figure 1 shows a schematic representation of the test apparatus. The specimens were cut from the cylindrical castings and machined to the aforementioned size. The samples were then metallographically polished, weighed, and fixed on a disc with the

Table 1 Chemical composition of the experimental alloys

Sr. no.	Specimen	Zn	Al	Cu	Mg	Si
		(Wt.%)				
1	Silicon-free alloy	*	37.5	2.5	0.2	…
2	Silicon-containing alloy	*	37.5	2.5	0.2	4

* Balance

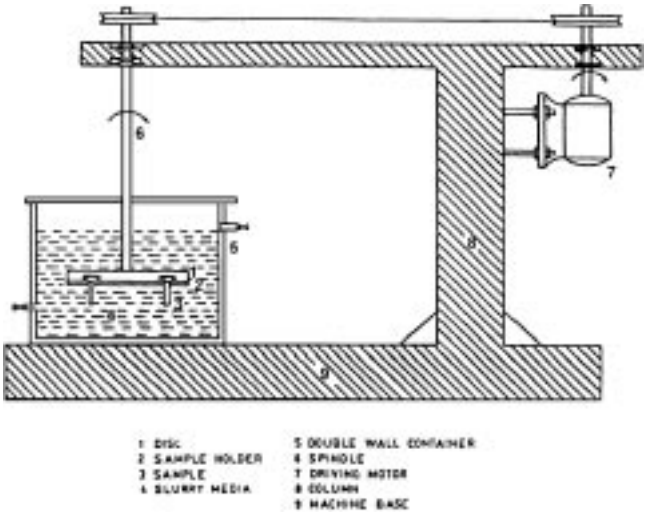

Fig. 1 A schematic representation of the slurry wear test apparatus

help of an adhesive. An electric motor was used to rotate the samples in a slurry over a range of traversal distances (15 to 500 km) and speeds (4.71 and 7.02 m/s). The slurry comprised 40% sand (212 to 300 μm) particles suspended in an electrolyte (prepared by mixing 5 cc concentrated sulfuric acid and 4 g sodium chloride in 10 L of water). The samples were cleaned thoroughly and weighed after the tests. A Mettler microbalance was used for weighing the samples.

2.3 Microscopic Studies

Microstructural investigations were carried out on 15 mm diameter, 10 mm thick samples machined from the castings. The samples were then polished as per standard metallographic techniques and etched with diluted aqua regia. A Leitz optical microscope was used for studying the microstructural features of the alloys.

Wear surfaces of typical specimens were cut and mounted on brass studs. The samples were then sputtered with gold and examined using a JEOL 35 CF scanning electron microscope (SEM, Japan Electron Optics Ltd., Tokyo). Subsurface analysis was carried out by cutting sections normal to the wear surfaces and mounting them in polyester resin. The samples were then metallographically polished, etched suitably, mounted on brass studs, and sputtered with gold prior to their SEM examination.

3. Results

Figure 2 reveals the microstructural features of the alloys. The alloy sample without silicon showed primary α dendrites

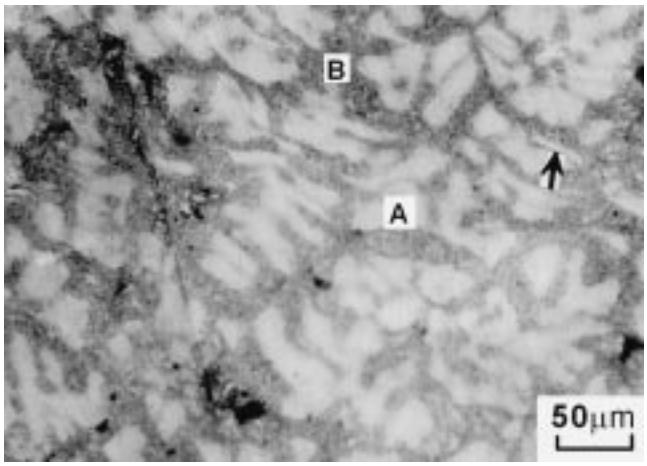

(a)

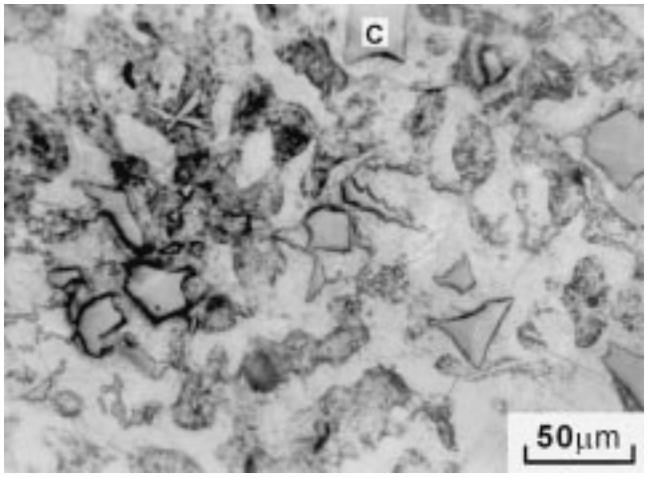

(b)

Fig. 2 Microstructure of (**a**) the silicon-free and (**b**) silicon-containing zinc-based alloys. (A: primary a, B: eutectoid $\alpha + \eta$, arrow: ε, and C: silicon particles)

surrounded by the eutectoid $\alpha + \eta$ and metastable ε phase (Fig. 2a, regions marked with A,B, and an arrow, respectively). Addition of silicon led to the formation of discrete particles of silicon (Fig. 2b, region marked C).

The wear rate of the samples has been plotted in Fig. 3 as a function of traversal distance at different speeds of rotation. The wear rate increased with distance in the beginning up to a specific distance, attained the maximum, and decreased thereafter at still longer distances in all cases. Increasing traversal speed led to higher wear rates irrespective of the alloy composition. Also, the silicon comprising alloy attained superior wear resistance (inverse of wear rate) to that of the one without the element (Fig. 3).

Wear surfaces of the silicon-free alloy are shown in Fig. 4. The surfaces of the samples tested at 4.71 m/s revealed the presence of abrasion grooves and indented regions along with fine pits (Fig. 4a). A magnified view clearly shows the areas (Fig. 4b, regions marked by a single arrow, A, and a double arrow, respectively). Identical features were observed when the tests were conducted at 7.02 m/s (Fig. 4c). A magnified view

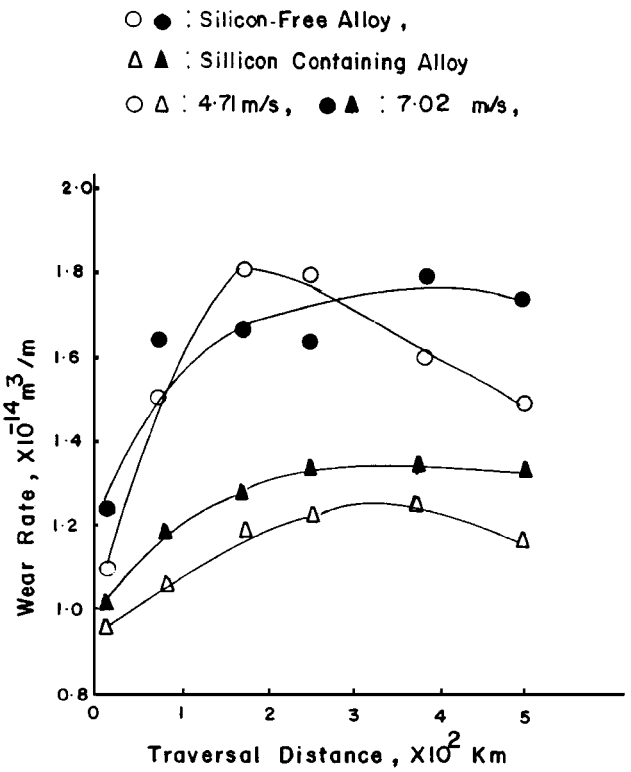

Fig. 3 Wear rate vs distance plots at different speeds

reveals the indented regions and pits (Fig. 4d, regions marked by A and a double arrow, respectively).

Figure 5 represents the features of the wear surfaces of the silicon-containing alloy. Abrasion grooves, indented regions, and pits were observed when tests were conducted at 4.71 m/s (Fig. 5a, regions marked by a single arrow, A, and a double arrow, respectively). The extent of surface damage increased at the higher speed (Fig. 5b), the nature of the damage remaining identical to that at 4.71 m/s (Fig. 5a). Figure 5b clearly reveals the abrasion grooves, indented regions, and pits (regions marked by a single arrow, A, and a double arrow, respectively). A typical example of the preferential (corrosive) attack of the slurry in the (silicon) particle/matrix interfacial regions is shown in Fig. 5c. The region marked B in the figure is the silicon particle, while the region marked with the triple arrow shows the interfacial attack of the medium.

Subsurface regions of the samples are shown in Fig. 6. Entrapment of fragmented sand particles in the indented regions was observed (Fig. 6a, region marked A). Regions marked by B and single and double arrows in Fig. 6b represent a typical indented region and microcracking in a silicon particle and in the alloy matrix, respectively.

4. Discussion

In slurry wear tests, the samples rotating in the slurry (liquid with solid suspension) experience the attack of the medium in the form of corrosion, erosion, and abrasion.[16–19] Corrosion of the specimens takes place because of the corrosive nature of the liquid (electrolyte) part of the slurry. Interfacial regions are quite prone to the corrosive attack of the medium due to the differential electrochemical potential of the two kinds of phases meeting together there.[16,19] This leads to the formation of corrosion pits. The corrosion products formed around the affected regions and the entrapped gaseous products in the regions delay/prohibit further corrosive attack of the medium, causing less material loss as long as they are present there.[16,19] The suspended solid mass in the liquid impinges the specimen surface due to the turbulence/hindrance created during the rotational motion of samples therein. Under these circumstances, indentation marks are created on the affected surface due to the impact generated by the indenting solid mass. A similar effect is also produced by the liquid droplets of the medium, although to a significantly lesser extent. It should be noted that compressive stressing occurs in the affected surface regions due to the impact of the impinging constituents of the slurry. The indented regions prior to cracking get work hardened and delay the process of material loss. However, when the generated degree of stressing exceeds a critical value, microcracking of the regions and, subsequently, material loss occur.

Fragmentation of the impinging solid particles also takes place, the particles becoming partially entrapped in the indentation marks and corrosion pits.[17,18] Entrapment of the (fragmented) impinging particles/corrosion products reduces the extent of overall material loss.

Abrasion is caused by the sliding motion of the solid mass on the specimen surface.[17,18] During the rotational movement of the sample in a slurry, abrasive damage occurs when the suspended mass does not get enough of an opportunity to impinge on the specimen surface in view of its large concentration and/or high speed of rotation beyond a limit in the medium.[17,18] Similar effects may also be produced when the suspended solid mass leaves the surface tangentially after impingement.

It should be mentioned that, in a slurry wear test by the sample rotation method, corrosive, erosive, and abrasive damage takes place on the specimen surface simultaneously or in quick succession. However, the predominance of either of the mentioned modes of material loss would depend on material-related factors such as the corrosion characteristics, hardness, interfacial characteristics, and strength of various microconstituents of a material; the adhering tendency of the corrosion products on the specimen surface; and so on.[16–22] As far as experimental parameters are concerned, slurry composition; corrosive nature of the (liquid part of) slurry; nature, shape, size, and content of the solid suspended mass; speed of rotation; and traversal distance play a major role in controlling the slurry wear behavior of a material.[16–24]

Material loss during slurry wear tests occurs in four stages,[16,19] namely, incubation period (stage I), accelerated material loss (stage II), decelerated erosion-corrosion (stage III), and steady-state wear (stage IV). The incubation period pertains to the time taken to initiate the attack of the slurry medium on the specimen surface by breaking/disrupting the passive oxide film there.[16,19] With the initiation of the destructive action of the slurry, a number of (fine) pits are

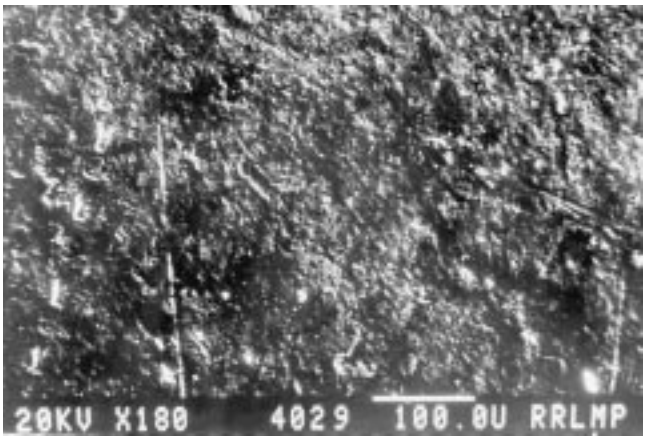

(a)

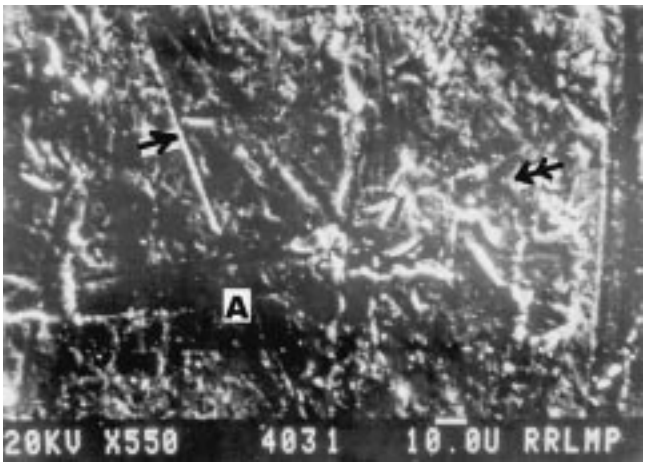

(b)

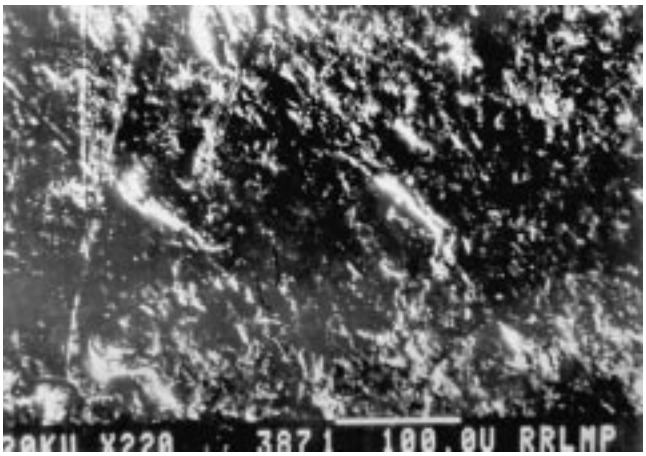

(c)

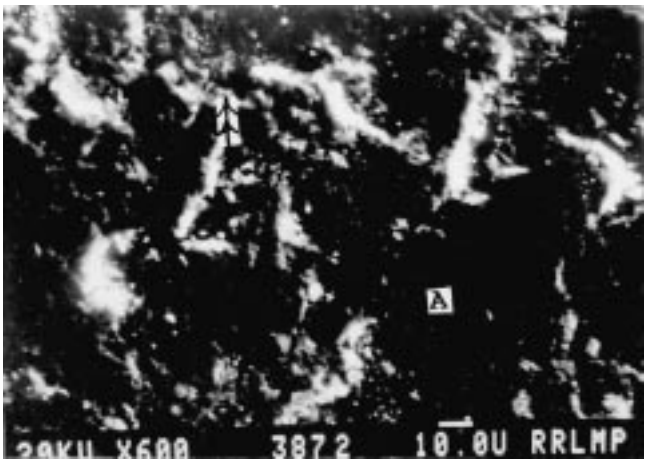

(d)

Fig. 4 Wear surfaces of the silicon-free zinc-based alloy after testing for 25 h at (**a**) and (**b**) 4.71 m/s and (**c**) and (**d**) 7.02 m/s. (Single arrow: abrasion grooves, A: indentation mark, and double arrow: pits)

formed on the specimen surface. This is followed by the formation of larger pits as the test progresses, leading to increasing material loss with test duration. As the surface damage becomes more severe, corrosion products around and the formation of gaseous products in the crevices reduce the extent and severity of further attack by the medium.[16,19] The corrosion products also tend to adhere to the affected regions, while the fragmented impinging solid mass suspended in the environment also gets entrapped in the indented regions/pits.[17,18] As a result, the wear rate decreases with test duration after attaining a maximum. In fact, the erosive-corrosive-abrasive attack of the medium, causing material loss, and the adhesion around and entrapment of corrosion products in the crevices/pits/indented regions, leading to a reduction in the extent of material loss, occur almost simultaneously. After some time, the two counterbalancing effects cause the occurrence of steady-state wear rate.

In the light of the above discussion, the observed wear response of the alloys in the present study will be analyzed now.

In this investigation, the electrolyte part of the slurry contained chloride and sulphate ions, which are quite corrosive in nature. As a result, no incubation period could be observed (Fig. 3). In fact, it might have been too short to be measured prior to making the first observation. Accelerated attack of the medium led to increased wear rate with distance and the attainment of the maximum. After traversing a still longer distance, the reduced rate of material loss was attributed to the decreasing severity of the corrosive attack of the medium in view of the formation and adherence of reaction/corrosion products and entrapment of fragmented sand particles[16,19] in the affected regions (Fig. 6a, region marked A).

Deterioration in the wear response of the alloys with increasing traversal speed (Fig. 3) could be attributed to more severe attack of the medium. The latter was also evident from deeper craters/pits formed on the specimen surface (Fig. 4c versus 4a and 5b versus 5a). The presence of hard silicon particles in the alloy system was able to resist the (erosive and abrasive) attack of the medium (Fig. 5c, region marked B, and Fig. 6b). This

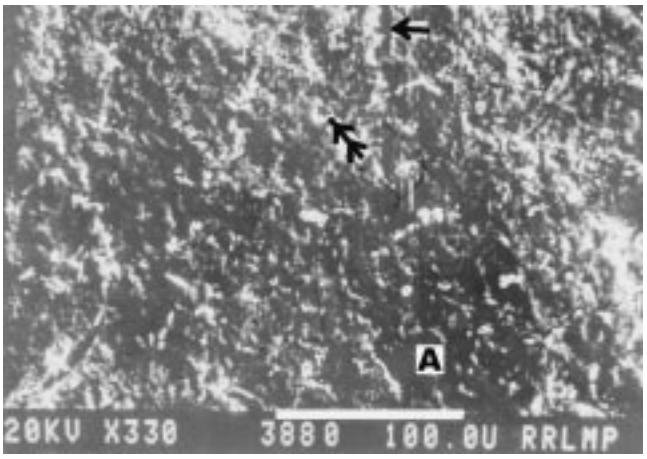

(a)

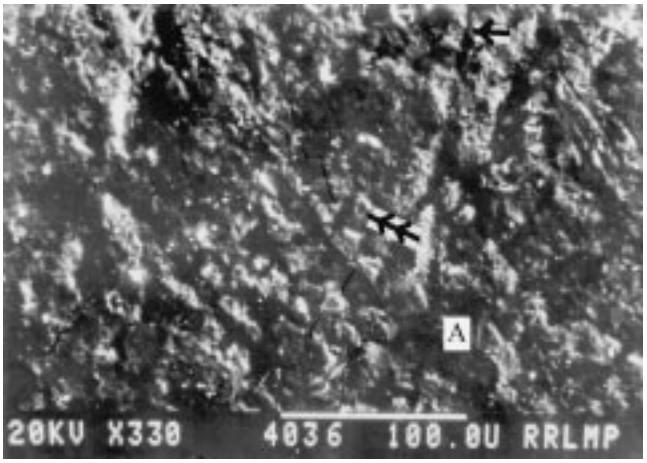

(b)

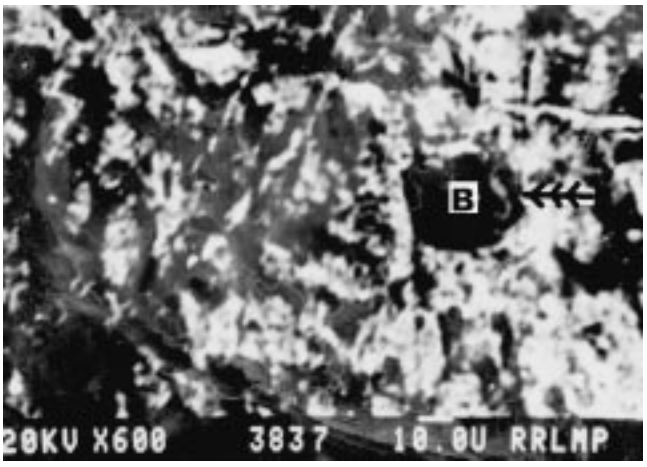

(c)

Fig. 5 Wear surfaces of the silicon-containing zinc-based alloy after testing for 25 h at (**a**) 4.71 m/s and (**b**) and (**c**) 7.02 m/s. (Single arrow: abrasion grooves, A: indentation mark, double arrow: pits, B: silicon particle, and triple arrow: interfacial attack)

led to the reduced wear rate of the silicon-containing alloy over the one without the element (Fig. 3).

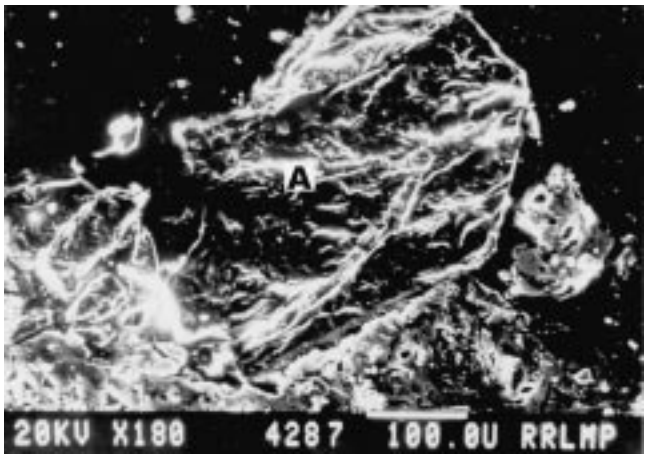

(a)

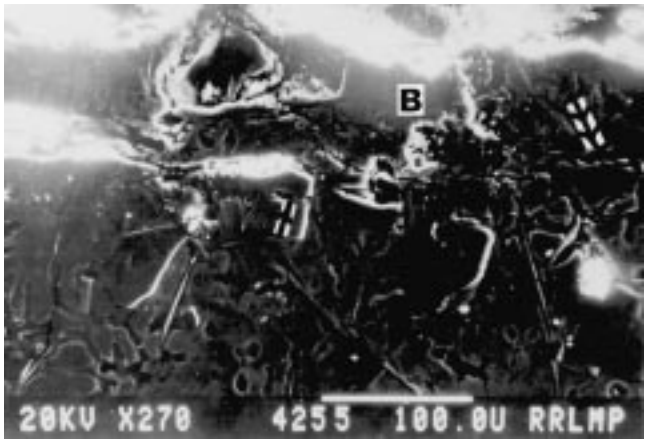

(b)

Fig. 6 Subsurface regions of (**a**) the silicon-free and (**b**) silicon-containing zinc-based alloys. (A: entrapped sand particle, B: indentation mark, single arrow: microcracking in silicon particles, and double arrow: microcracking in the alloy matrix)

5. Conclusions

- Wear rate of the samples increased with distance in the beginning, attained a maximum, and decreased thereafter at longer traversal distances.
- Higher traversal speed led to larger wear rates irrespective of the alloy composition.
- Addition of silicon improved the wear resistance (inverse of wear rate) of the alloy system.
- Corrosion, erosion, and abrasion modes of material removal were observed to be the operating wear mechanisms in this investigation.

References

1. E.J. Kubel, Jr.: *Adv. Mater. Proc.*, 1987, vol. 132, pp. 51-57.

2. M.J. Barber and P.E. Jones: *Foundry Trade J.*, 1980, vol. 148, pp. 114-31.
3. D. Apelian, M. Paliwal, and D.C. Herrschaft: *J. Met.*, 1981, vol. 133, pp. 12-20.
4. B.K. Prasad, S. Das, A.K. Jha, O.P. Modi, R. Dasgupta, and A.H. Yegneswaran: *Proc. XI Nat. Convention of Mechanical Engineers*, A.D. Telang and H.B. Khurasia eds., Nov. 25–26, 1995, Bhopal, India, The Institution of Engineers (I), Bhopal, India, 1995, pp. M1-M9.
5. J. Zahavi and H.J. Wagner: *Proc. Symp. Corrosion-Erosion/Behavior of Materials*, Fall Meeting of TMS-AIME, St. Louis, MO, Oct. 17–18, 1978, K. Natesan, ed., AIME, Warrendale, PA, 1978, pp. 226-34.
6. B.K. Prasad, A.K. Patwardhan, and A.H. Yegneswaran: *J. Mater. Eng. Perf.*, 1998, vol. 7, pp. 130-35.
7. B.K. Prasad, A.K. Patwardhan, and A.H. Yegneswaran: *Scripta. Mater.*, 1997, vol. 37, pp. 323-28.
8. B.K. Prasad: *Z. Metallkd.*, 1997, vol. 88, pp. 929-33.
9. B.K. Prasad, K. Venkateswarlu, O.P. Modi, S. Das, A.K. Jha, R. Dasgupta, and A.H. Yegneswaran: *Proc. Int. Conf. Aluminium (INCAL-98)*, Feb. 11–13, 1998, D.H. Sastry, S. Subramanian, K.S.S. Murthy, and K.P. Abraham, eds., The Aluminium Association of India, New Delhi, 1998, vol. 2, pp. 9-16.
10. M.A. Dellis, J.K. Keustermans, and F. Delannay: *Mater. Sci. Eng. A*, 1991, vol. 135A, pp. 253-57.
11. L.D. Bailey, S. Dionne, and S.H. Lo: *Proc. Fundamental Relationship between Microstructure and Properties of Metal Matrix Composites*, P.K. Liaw and M.N. Gungor, eds., TMS, Warrendale, PA, 1990, pp. 23-25.
12. S. Muthukumaraswamy and S. Seshan: Composites, 1995, vol. 26, pp. 387-93.
13. S.H.J. Lo, S. Dionne, M. Sahoo, and H.M. Hawthorne: *J. Mater. Sci.*, 1992, vol. 27, pp. 5681-91.
14. H.X. Zhu and S.K. Liu: *Composites*, 1993, vol. 5, pp. 437-42.
15. N.B. Dahotre, T.D. McCay, and M.H. McCay: *J. Met.*, 1990, vol. 42, pp. 44-47.
16. M. Saxena, O.P. Modi, B.K. Prasad, and A.K. Jha: *Wear*, 1993, vol. 169, pp. 119-24.
17. R. Dasgupta, B.K. Prasad, A.K. Jha, O.P. Modi, S. Das, and A.H. Yegneswaran: *Wear*, 1997, vol. 213, pp. 41-46.
18. R. Dasgupta, B.K. Prasad, A.K. Jha, O.P. Modi, S. Das, and A.H. Yegneswaran: *Wear*, 1997, vol. 209, pp. 255-62.
19. O.P. Modi, M. Saxena, B.K. Prasad, A.H. Yegneswaran, and M.L. Vaidya: *J. Mater. Sci.*, 1992, vol. 27, pp. 3897-3902.
20. S. Turene, D. Simard, and M. Fiset: *Wear*, 1991, vol. 149, pp. 187-97.
21. S. Turene, Y. Chatigny, D. Simard, S. Caron, and J. Masounave: *Wear*, 1990, vol. 141, pp. 147-58.
22. A.V. Levy: *Corrosion*, 1995, vol. 51, pp. 872-83.
23. Deonath and T.K.G. Namboodhiri: *Composites*, 1988, vol. 19, pp. 237-43.
24. Y. Li, G.T. Burstein, and I.M. Hutchings: *Wear*, 1995, vol. 181–183, pp. 70-79.